Supporting information for *Chemical Communications*

Colorimetric fluoride sensors based on deprotonation of pyrrole-hemiquinone compounds

Quanguo Wang, Yongshu Xie*, Yubin Ding, Xin Li, and Weihong Zhu*

Key Laboratory for Advanced Materials and Institute of Fine Chemicals, East China University of Science and Technology, Shanghai 200237, P. R. China

Experimental Section

General

Commercial available solvents and reagents were used without further purification. Deuterated solvents for NMR measurements were obtained from Aldrich. UV/Vis absorption spectra were measured using a Varian Cary 100 spectrophotometer, with a quartz cell (path length = 1 cm). ^{1}H NMR spectra were obtained on a Bruker AVANCE spectrometer (400 or 500 MHz). Spectrophotometric titrations were performed on 1.0×10^{-5} M solutions of **1** and **2** in CH_2Cl_2 or DMSO (analytical grade). Typically, aliquots of a freshly prepared alkylammonium salt standard solution of the envisaged anion (CH_3COO^-, F^-, Cl^-, Br^-, or I^-) were added, and the UV-vis spectra were recorded. ^{1}H NMR titrations were carried out in $CDCl_3$ or DMSO-d_6 solution.

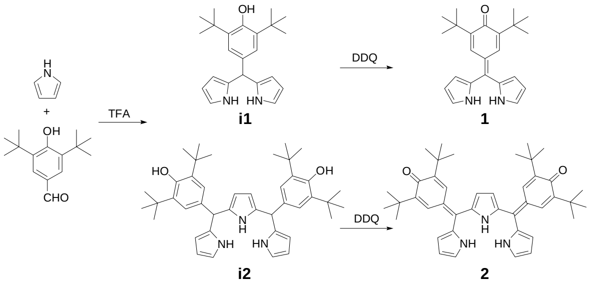

Scheme S1 Synthesis of sensors **1** and **2**.

Synthesis of i1

153 uL of TFA was added with syringe to the mixture of pyrrole (13.8 mL, 0.20 mol) and 3,5-Di-*tert*-butyl-4-hydroxybenzaldehyde (469 mg, 2.0 mmol). After stirred at room temperature for 30 min, saturated $NaHCO_3$ (30 mL) was added, and then the mixture was extracted with CH_2Cl_2 (30 mL × 2). The combined organic phase was washed with water, dried over Na_2SO_4, filtered and evaporated. Pyrrole was recycled by distillation under reduced pressure and the residue was purified by a silica gel column to afford the desired product dipyrromethane **i1** (479 mg, yield: 68%). ^{1}H NMR ($CDCl_3$, Bruker 500 MHz, 298K): δ 1.39 (s, 18H, -$C(CH_3)_3$), 5.13 (s, 1H, phenolic-OH), 5.36 (s, 1H, -CH), 5.92 (s, 2H, pyrrolic), 6.15 (d, J = 2.8 Hz, 2H, pyrrolic), 6.68 (s, 2H, pyrrolic), 7.00 (s, 2H, phenyl), 7.89 (br, 2H, -NH).

Synthesis of i2

TFA (2.2 mmol, 170 µL) was added to the mixture of 3, 5-Di-*tert*-butyl-4-hydroxy-benzaldehyde (22 mmol, 5.2 g) and pyrrole (100 mmol, 7.6 mL). After stirred at room temperature for 5 min under nitrogen, aqueous NaOH (0.1 M, 20 mL) was added. and then the mixture was extracted with CH_2Cl_2 (50 mL × 2). The combined organic phase was washed with water, dried over Na_2SO_4, filtered and evaporated. Pyrrole was recycled by distillation under reduced pressure. Chromatography of the resulting oil (silica gel, CH_2Cl_2/petroleum ether 1:4) afforded the product **i2** (1.23g, 18%). ^{1}H NMR ($CDCl_3$, 500 MHz, 298K): δ 1.37 (m, 36H, -$C(CH_3)_3$), 5.11 (s, 2H, phenolic-OH), 5.27 (s, 2H, -CH), 5.75-5.80 (m, 2H, pyrrolic), 5.85 (d, J = 2.1 Hz, 2H, pyrrolic), 6.07-6.12 (m, 2H, pyrrolic), 6.62-6.67 (m, 2H, pyrrolic), 6.97 (s, 4H, phenyl), 7.74 (br, 1H, central NH), 7.89 (br, 2H, peripheral NH).

Synthesis of 1

DDQ (111 mg, 0.49 mmol) was added to a solution of **i1** (114 mg, 0.33 mmol) in 50 mL of CH_2Cl_2. The mixture was stirred at room temperature for 30 min and then directly purified by silica gel column (Eluent: CH_2Cl_2 : MeOH) to afford the crude product **1** which was recrystallized from CH_2Cl_2 and *n*-hexane (71 mg, yield: 63%). mp. 235-236 °C. IR ν_{max} (KBr)/cm^{-1}: 3432, 3392, 3270, 2962, 1610, 1572, 1535, 1471, 1446, 1401, 1384, 1358, 1335, 1128, 1115, 1041, 1021, 986, 630, 579, 532. ^{1}H NMR (DMSO-d_6, Bruker 500 MHz, 298K): δ 1.26 (s, 18H, -$C(CH_3)_3$), 6.33-6.42 (m, 2H, pyrrolic), 6.44-6.52 (m, 2H, pyrrolic), 7.18-7.27 (m, 2H, pyrrolic), 7.36 (s, 2H, hemiquinone), 11.47 (s, 2H, -NH). ^{13}C NMR (DMSO-d_6, Bruker 75 MHz, 298K): δ 183.76, 143.59, 139.73, 132.34, 129.82, 125.29, 121.87, 119.11, 110.77, 34.78, 29.27.HRMS (ESI): calcd for $C_{23}H_{29}N_2O$ $[M]^+$, 349.2280; found, 349.2273.

Synthesis of 2

DDQ (108 mg, 0.48 mmol) was added to a solution of **i2** (100 mg, 0.16 mmol) in 50 mL of CH_2Cl_2. The mixture was stirred at room temperature for 30 min and then directly purified by silica gel column (Eluent: PE : CH_2Cl_2). The crude product was further purified by another silica gel column (Eluent: PE : CH_2Cl_2 = 1 : 1, 1% Et_3N), and then recrystallized from methanol and water to afford the desired product **2** (61 mg, yield: 62%). mp. > 280 °C. IR ν_{max} (KBr)/cm^{-1}: 3424, 2954, 1610, 1572, 1539, 1484, 1447, 1397, 1386, 1359, 1334, 1295, 1255, 1232, 1203, 1146, 1091, 1045, 1024, 987, 931, 881, 836, 739, 638, 534. ^{1}H NMR (DMSO-d_6, Bruker 500 MHz, 298K): δ 1.26 (s, 18H, -$C(CH_3)_3$), 1.28 (s, 18H, -$C(CH_3)_3$), 6.40-6.43 (m, 2H, pyrrolic), 6.66 (m, 2H, pyrrolic), 6.75 (d, J = 2.0 Hz, 2H, pyrrolic), 7.29 (m, 2H, pyrrolic), 7.39 (d, J = 2.3 Hz, 2H, hemiquinone), 7.52 (d, J = 2.2 Hz, 2H, hemiquinone), 11.45 (s, 2H, peripheral NH), 11.81 (s, 1H, central NH). ^{13}C NMR (DMSO-d_6, Bruker 75 MHz, 298K): δ 184.71, 145.14, 144.43, 138.35, 135.71, 133.02, 132.20, 130.36, 125.83, 124.77, 120.33, 119.57, 111.62, 35.40, 35.32, 29.79, 29.65. HRMS (ESI): calcd for $C_{42}H_{52}N_3O_2$ $[M]^+$, 630.4060; found, 630.4066.

DFT calculations

Density functional theory (DFT) calculations were carried out by the Gaussian03 program,[1] using the hybrid B3LYP functional and 6-31G(d) basis set. The geometries of mono- and di-deprotonated species, **2b** and **2c** (Fig. S9), were optimized in vacuum, and subsequent single point calculations as well as time-dependent density functional theory (TDDFT) calculations were performed with the polarizable continuum model (PCM)[2] to take into account the solvent effect of DMSO. The results are presented in Table S1 and Fig. S9.

To gain insights of the isomerization behaviors of compound **1** and **2**, density functional theory (DFT) calculations are also carried out by the Gaussian03 program, using the hybrid B3LYP functional and 6-31G(d) basis set. The geometries of compound **1** and **2** are optimized in vacuum, and subsequent single point calculations are performed with solvent effects taken into account by the polarizable continuum model (PCM), using $CHCl_3$ and DMSO as solvents, respectively. The energies are compared between isomers, and the energy differences are listed in Table S2.

References

1 M. J. Frisch, G. W. Trucks, H. B. Schlegel, G. E. Scuseria, M. A. Robb, J. R. Cheeseman, J. A. Montgomery, Jr., T. Vreven, K. N. Kudin, J. C. Burant, J. M. Millam, S. S. Iyengar, J. Tomasi, V. Barone, B. Mennucci, M. Cossi, G. Scalmani, N. Rega, G. A. Petersson, H. Nakatsuji, M. Hada, M. Ehara, K. Toyota, R. Fukuda, J. Hasegawa, M. Ishida, T. Nakajima, Y. Honda, O. Kitao, H. Nakai, M. Klene, X. Li, J. E. Knox, H. P. Hratchian, J. B. Cross, V. Bakken, C. Adamo, J. Jaramillo, R. Gomperts, R. E. Stratmann, O. Yazyev, A. J. Austin, R. Cammi, C. Pomelli, J. W. Ochterski, P. Y. Ayala, K. Morokuma, G. A. Voth, P. Salvador, J. J. Dannenberg, V. G. Zakrzewski, S. Dapprich, A. D. Daniels, M. C. Strain, O. Farkas, D. K. Malick, A. D. Rabuck, K. Raghavachari, J. B. Foresman, J. V. Ortiz, Q. Cui, A. G. Baboul, S. Clifford, J. Cioslowski, B. B. Stefanov, G. Liu, A. Liashenko, P. Piskorz, I. Komaromi, R. L. Martin, D. J. Fox, T. Keith, M. A. Al-Laham, C. Y. Peng, A. Nanayakkara, M. Challacombe, P. M. W. Gill, B. Johnson, W. Chen, M. W. Wong, C. Gonzalez, J. A. Pople, *Gaussian 03*, *Revision D.01*; Gaussian, Inc., Wallingford CT, 2004.

2 (*a*) M. T. Cancès, B. Mennucci and J. Tomasi, *J. Chem. Phys.*, 1997, **107**, 3032; (*b*) M. Cossi, G. Scalmani, N. Rega and V. Barone, *J. Chem. Phys.*, 2002, **117**, 43.

Tables and figures

Table S1. Calculated TDDFT excitation energies (eV, nm), oscillator strengths (*f*), and composition in terms of molecular orbital contributions

Compound	State	Composition [a]	E(eV, nm)	*f*
2b	S_1	H→L(83%)	1.72, 720.4	0.2539
	S_2	H1→L(70%)	2.25, 552.2	0.9865
2c	S_1	H→L(82%)	1.83, 675.9	0.4371
	S_2	H1→L(80%)	1.94, 638.3	0.2695

[a] H = HOMO, L = LUMO, H1 = HOMO-1.

Table S2. Calculated energy differences between the tautomeric isomers in various solvents (in kJ/mol)

Solvent	$E_{1a} – E_1$	$E_{2a} – E_2$
Vacuum	4.75	-9.50
$CHCl_3$	25.15	10.29
DMSO	34.49	20.59

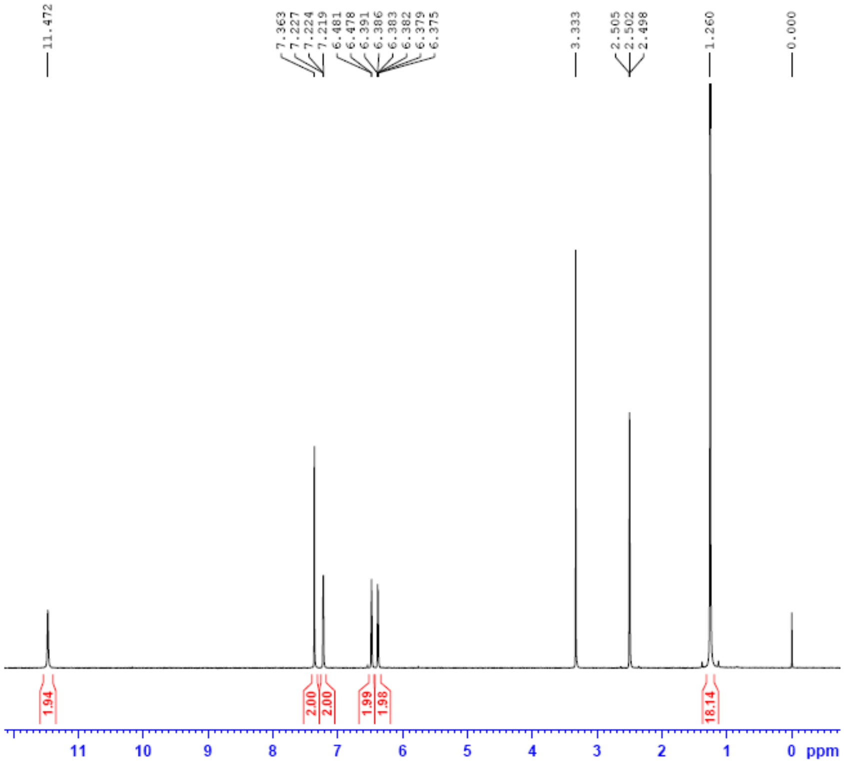

Fig. S1. The ^{1}H NMR spectrum of **1** in DMSO-d_6.

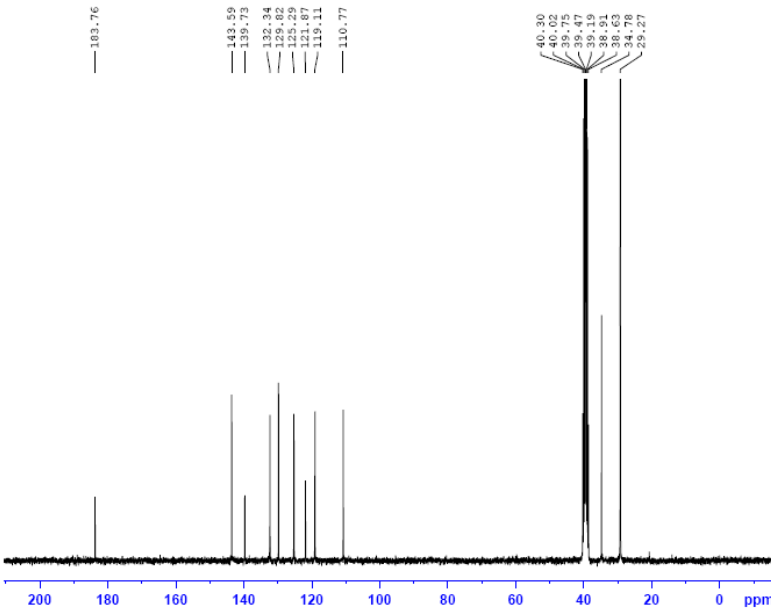

Fig. S2. The ^{13}C NMR spectrum of **1** in DMSO-d_6.

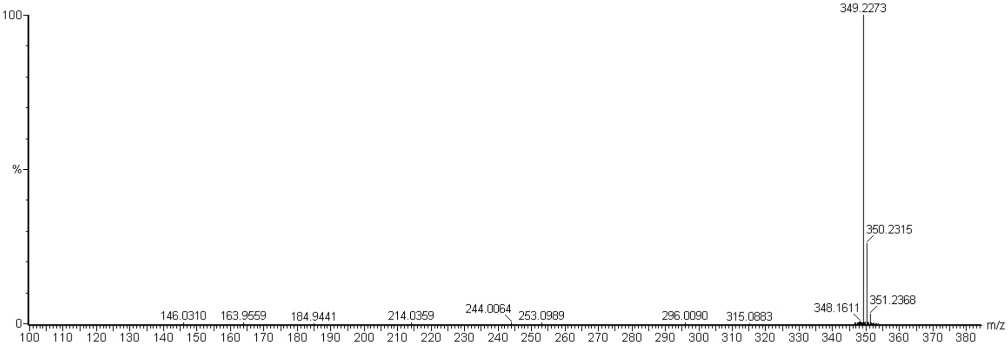

Fig. S3. ESI HRMS of **1** in MeOH.

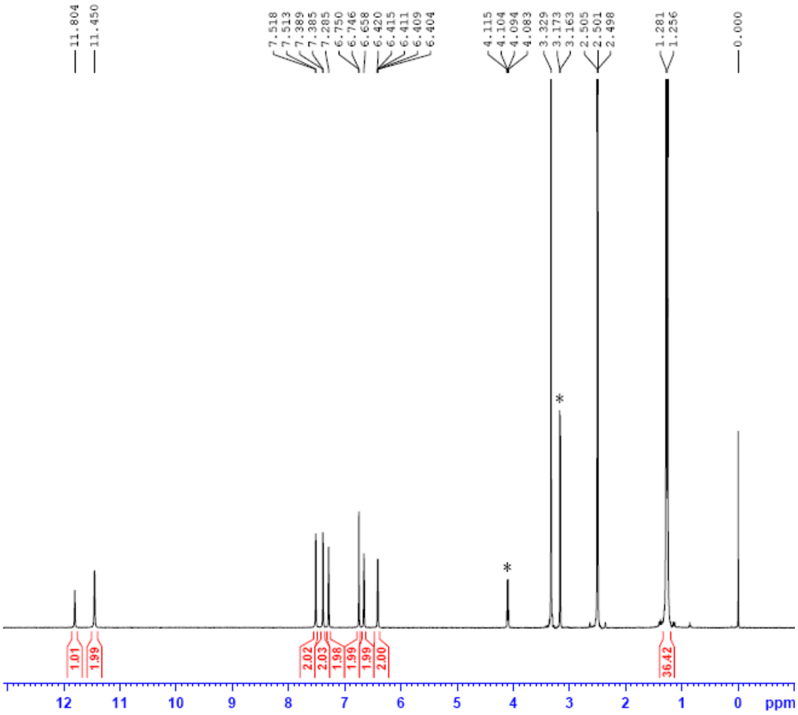

Fig. S4. The ^{1}H NMR spectrum of **2** in DMSO-d_6 (Asterisks represent the peaks of methanol).

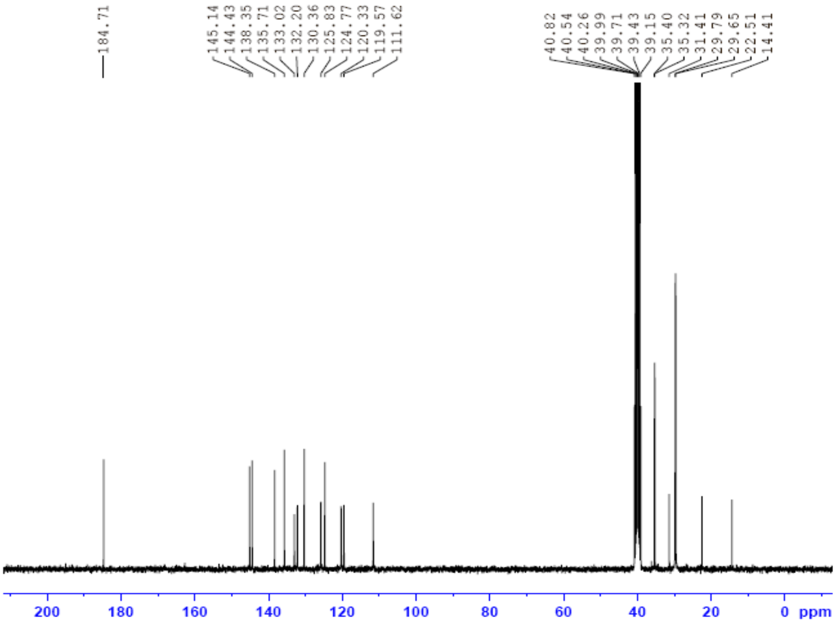

Fig. S5. The ^{13}C NMR spectrum of **2** in DMSO-d_6.

Fig. S6. ESI-HRMS of **2** in MeOH.

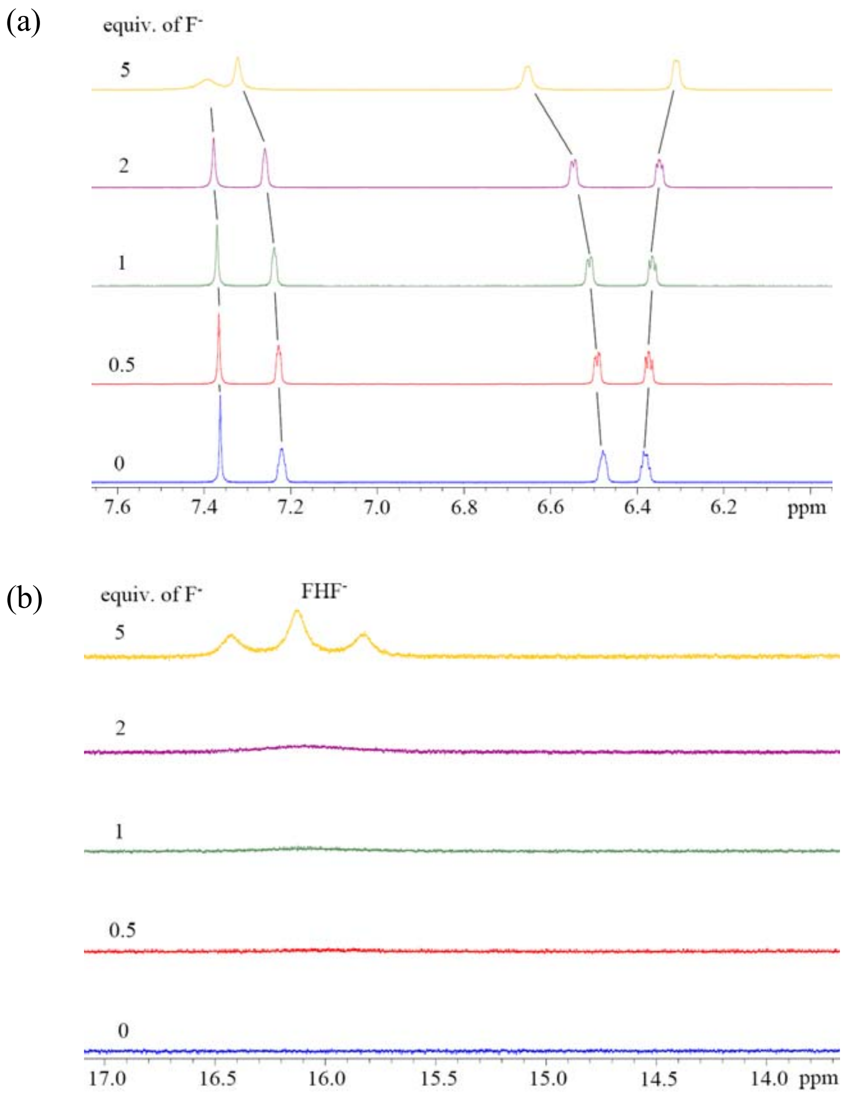

Fig. S7. ^{1}H NMR spectra of **1** (11.5 mM) with fluoride anion (TBA salt) in DMSO-d_6 (0-5 *eq*).

Fig. S8. Color changes of **2** (15 μM) in DMSO upon addition of 40 *eq*. (Top) and 150 *eq*. of anions (Bottom).

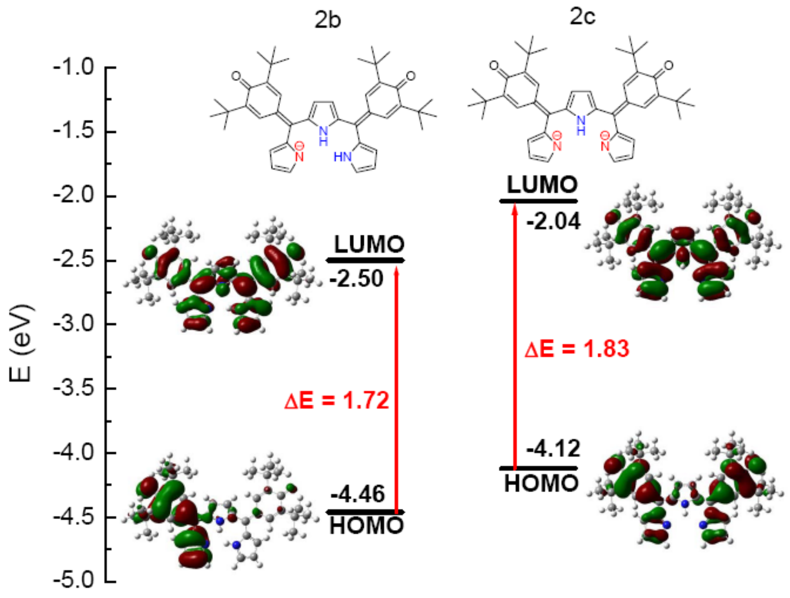

Fig. S9. Calculated HOMO and LUMO levels for mono- and di-deprotonated species of **2**.

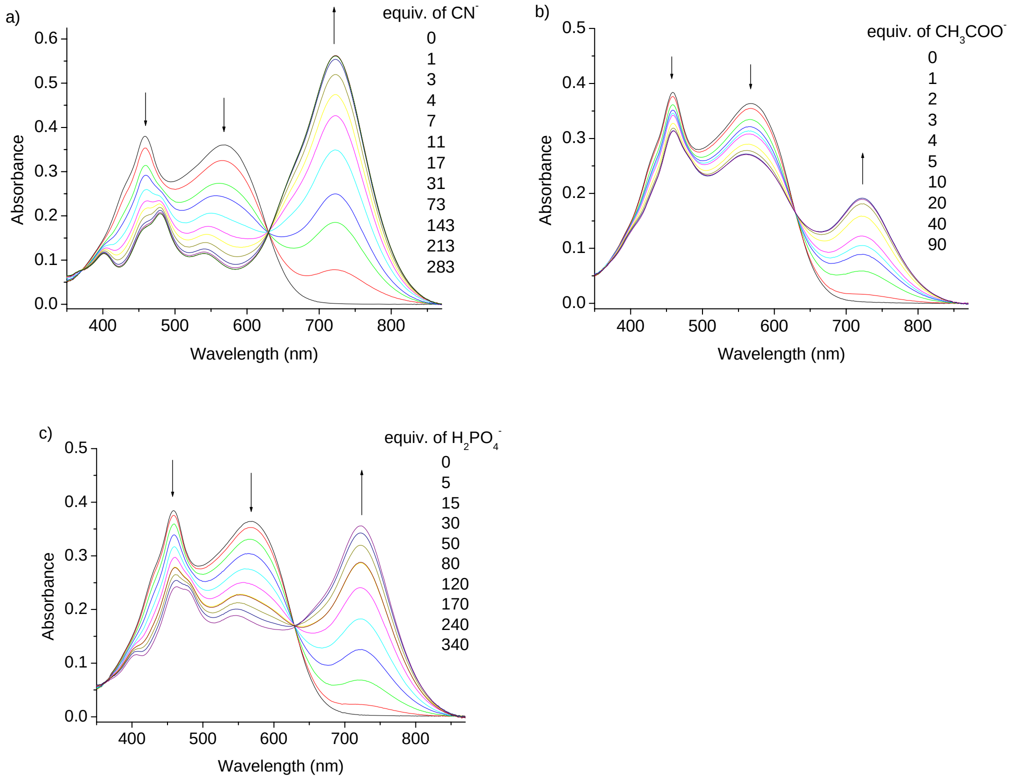

Fig. S10. UV-vis spectral changes of **2** (10 µM in DMSO) observed upon the addition of anions. a) CN^-, b) CH_3COO^-, and c) $H_2PO_4^-$ (TBA salt).

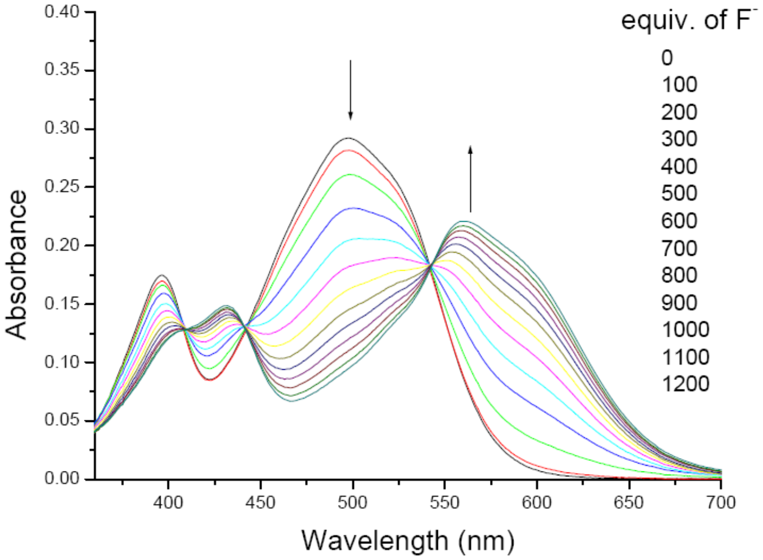

Fig. S11 UV-vis spectral changes of **1** (10 μM in DMSO/H_2O (29:1, v/v)) observed upon addition of 0-1200 *eq.* of F^- (TBA salt).

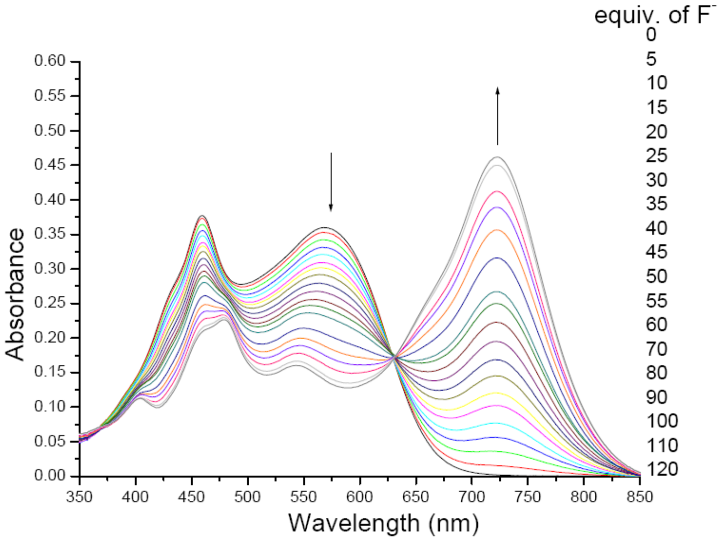

Fig. S12 UV-vis spectral changes of **2** (10 μM in DMSO/H_2O (29:1, v/v)) observed upon addition of 0-120 *eq.* of F^- (TBA salt).

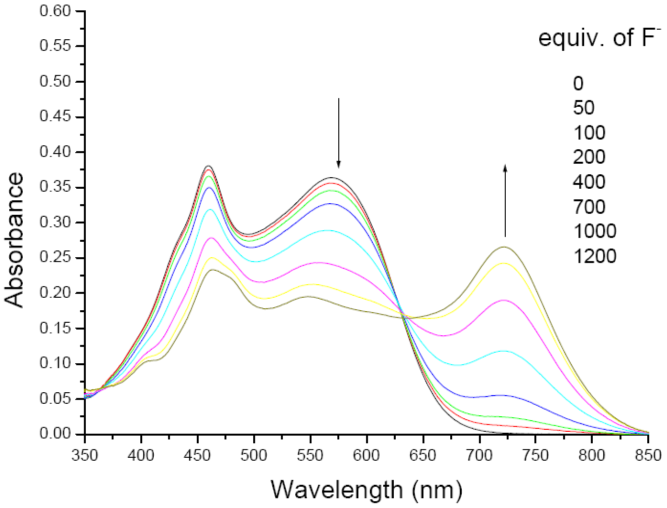

Fig. S13 UV-vis spectral changes of **2** (10 µM in DMSO/H_2O (9:1, v/v)) observed upon addition of 0-1200 *eq.* of F^- (TBA salt).

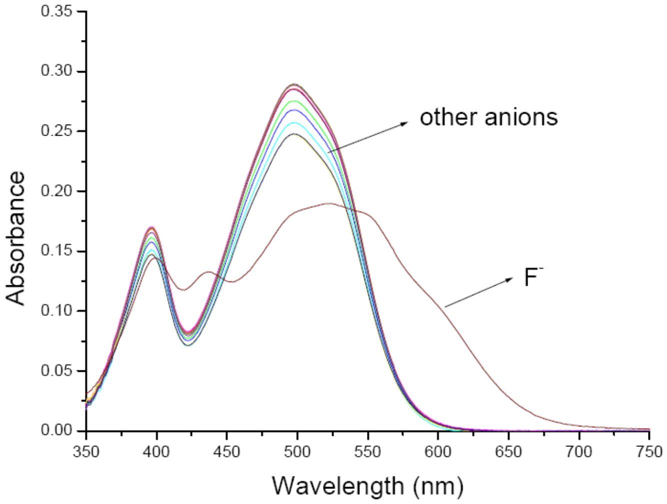

Fig. S14 UV-vis spectral changes of **1** (10 µM in DMSO/H_2O (29:1, v/v)) observed upon addition of 500 *eq.* of various anions (TBA salt).

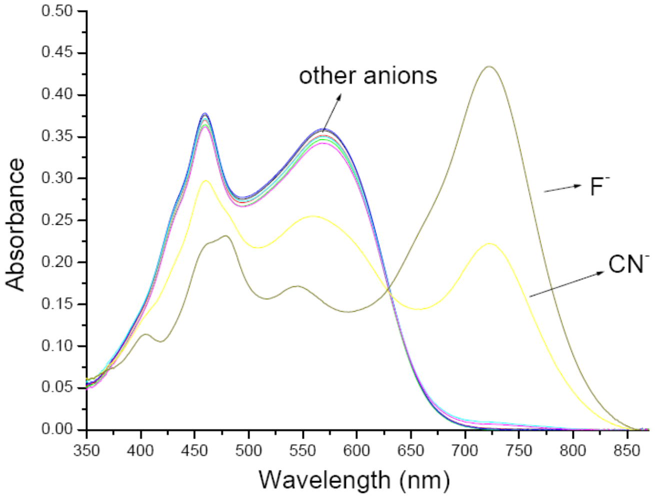

Fig. S15 UV-vis spectral changes of **2** (10 µM in DMSO/H_2O (29:1, v/v)) observed upon addition of 100 *eq.* of various anions (TBA salt).

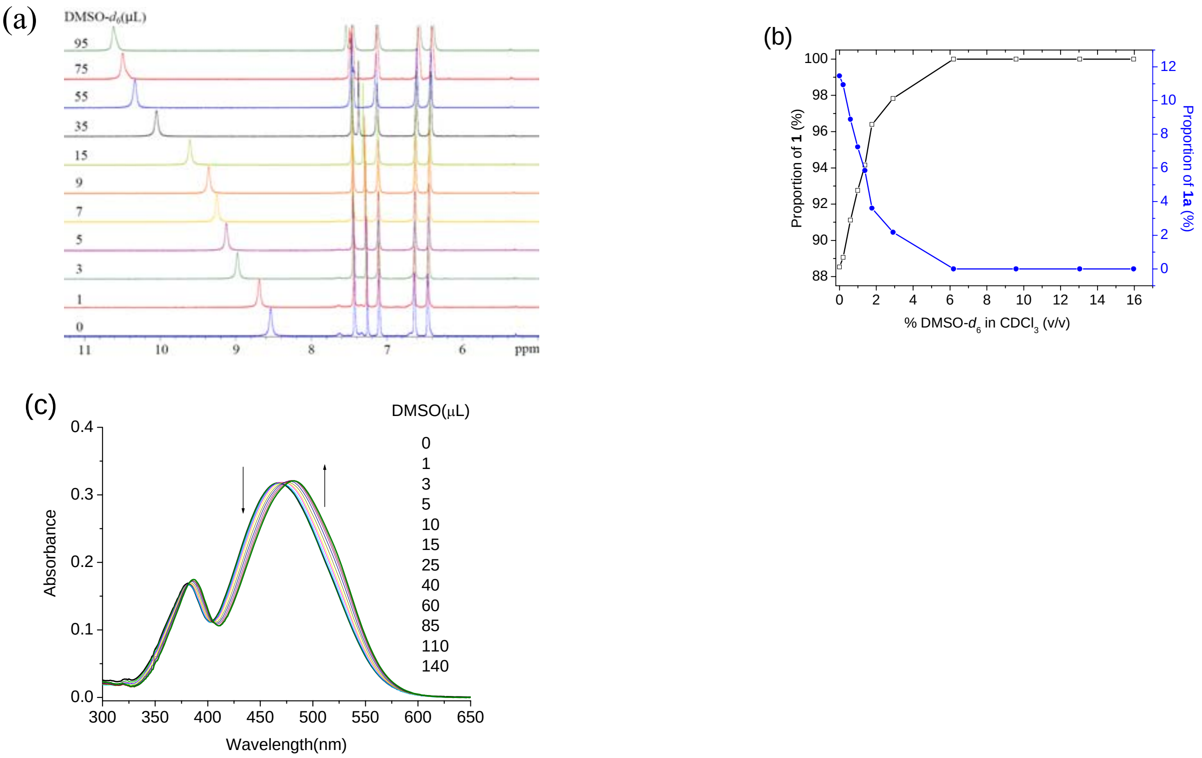

Fig. S16. (a) ^{1}H NMR spectral changes of **1** (11.5 mM) in $CDCl_3$ upon addition of DMSO-d_6, (b) the corresponding percentages of tautomeric isomers **1** and **1a** calculated from the ratio of related peak areas in the ^{1}H NMR spectra, and (c) UV-vis spectral changes of **1** (10 μM in CH_2Cl_2) upon addition of DMSO.

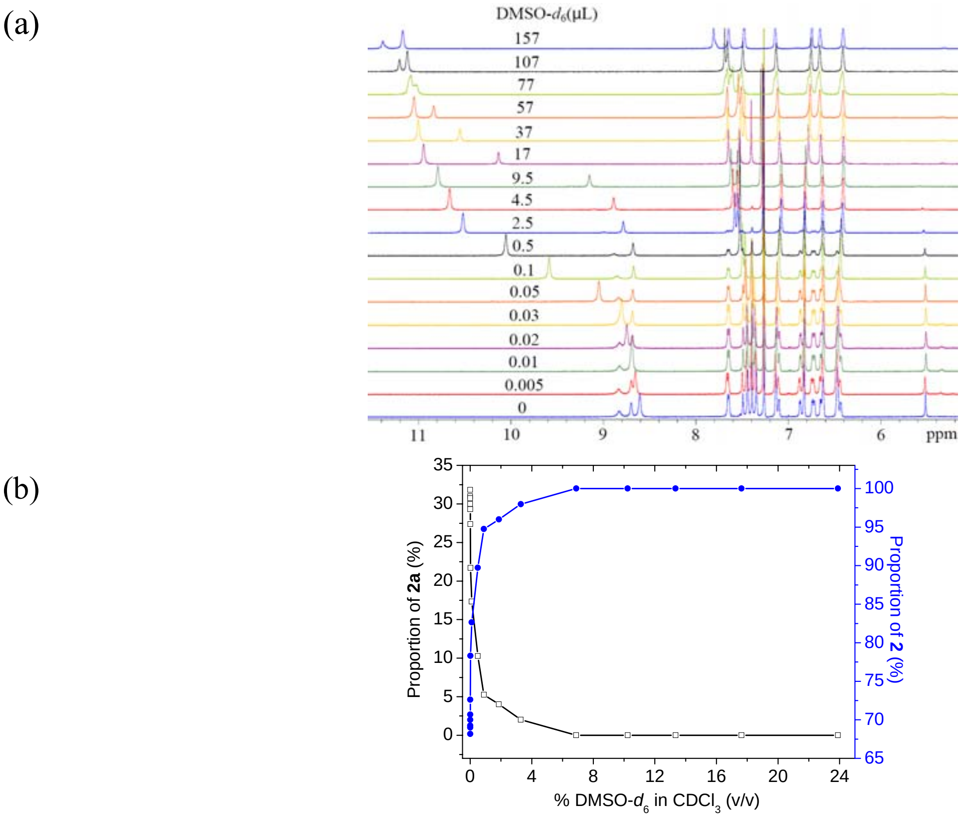

Fig. S17. (a) ^{1}H NMR spectral changes of **2** (6.4 mM) in $CDCl_3$ (0.5 mL) upon addition of DMSO-d_6, (b) the corresponding percentages of tautomeric isomers **2** and **2a** calculated from the ratio of related peak areas in the ^{1}H NMR spectra.

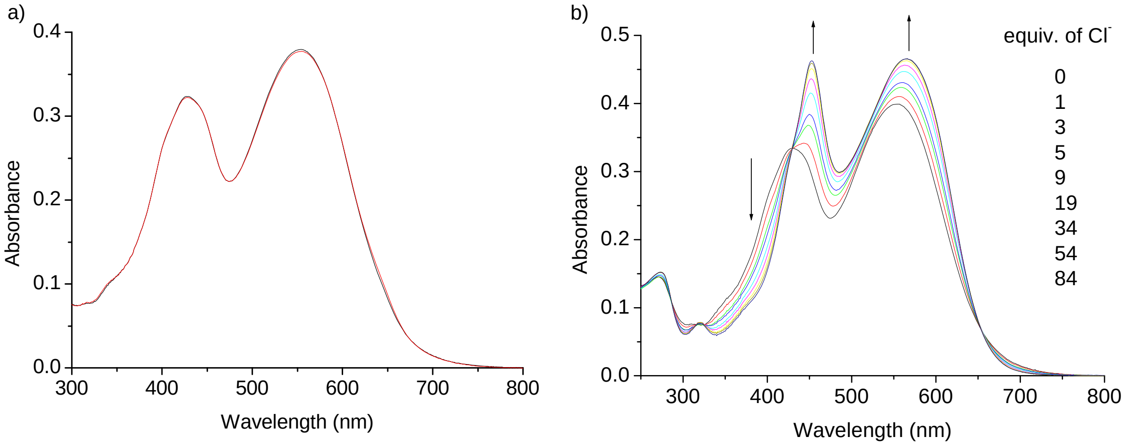

Fig. S18. UV-vis spectral changes of **2** (10 μM) observed upon addition of a) 100 *eq*. of Cl^- (TBA salt) in DMSO; b) 0-84 *eq*. of Cl^- (TBA salt) in CH_2Cl_2.

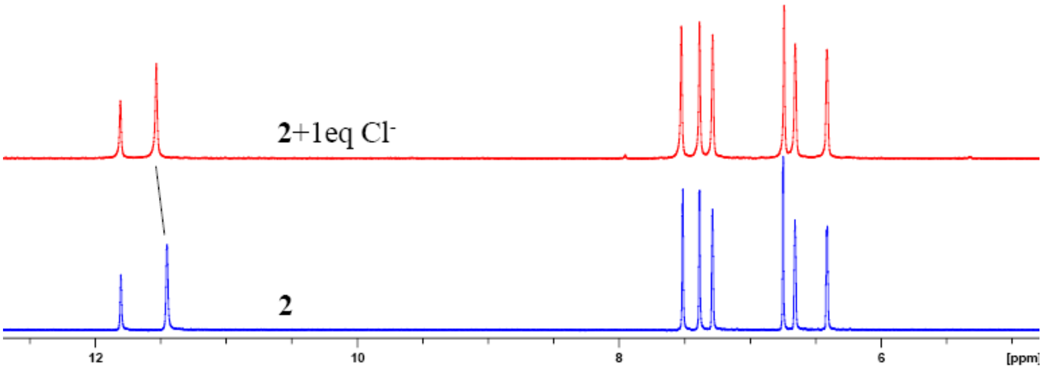

Fig. S19. ^{1}H NMR spectrum change of **2** (6.4 mM) upon addition of TBACl (1 *eq*) in DMSO-d_6.